5. Fore-and-Aft Vibration of Superstructure Located at Aftership

Tomoyuki HIROWATARI*, *Member* and Kohei MATSUMOTO*, *Member*

(From J.S.N.A. Japan, Vol. 118, Dec. 1965.)

Summary

The large ship recently built in Japan are generally of the type with the entire superstructure aft, and for these vessels special attention should be paid to vibration especially to the fore-and-aft vibration of superstructures.

The authors have carried out some experimental and theoretical investigation on these phenomena, and the following results have been obtained.

(1) In full scale measurements, there were several peak groups recognized in the vicinities of 400~600 c/m and 800~1,000 c/m, of these the lowest have possibility of resonating with the so-called blade frequencies.

(2) Measured mode curves had shown interesting characteristics.

(3) Some qualitative investigations have been made on these experimental data, and it becomes clear that the coupled motion of the main hull, the elastic support at the base deck of superstructure and the dodger have a great deal of influence upon the vibratory characteristics of superstructure.

(4) A method of predicting the lowest natural frequency of superstructure by the use of electronic computer has been obtained.

1. Introduction

Most of huge vessels recently built in Japan are of a type with the entire superstructure aft, and the bridge of this kind of vessels has to be positioned as high as possible for navigational reasons. On these ships, the troublesome fore-and-aft vibration of the superstructure has sometimes occurred due to resonance with the so-called blade frequency, because the higher it is, the lower the natural frequencies are. In order to avoid this trouble, it is necessary to investigate the vibratory characteristics of superstructures of this kind and obtain some useful method for predicting their critical frequencies at the stage of designing.

This paper describes the vibratory characteristics of such superstructures obtained on full-scale measurements, some qualitative studies of them, and proposes a method for determining the natural frequencies of the fore-and-aft vibration.

* Technical Research Laboratory, Hitachi Shipbuilding & Engineering Co., Ltd.

2. Full-scale Vibration Measurements

2.1 *Test Ship.*

Full-scale vibration measurements were carried out on nine newly built huge vessels with the entire superstructure aft, called in this paper A, B, C and so forth. The main dimensions and particulars of the test ships are shown in Table 1 and the dimensions of the superstructures are given in Table 2.

2.2 *Experimental Method.*

The vibration measurements were two kinds: measurements at a pier by means of a vibration exciter installed on some deck of the superstructure, and measurements during her trial runs.

A remote recording system consisting of accelerometer pickups, amplifiers and recording oscillographs was used to measure the vibrations of superstructure and main hull

Table 1 Principal Particulars of Test Ship.

Ship Name	Ship Kind	L×B×D (m)	D.W. (kT)	Main Engine	Revolution (r.p.m)	No. of Propellr Blades	Note
A	Tanker	246.00×40.20×21.80	99,655	Hitachi B&W 1284-VT2BF-180	108	5	Conventional Type Superstructure
B	Tanker	246.00×40.20×21.80	103,929	Hitachi B&W 1084-VT2BF-180	108	6	ditto
C	Ore Carrier	241.00×36.80×17.90	82,056	Hitachi B&W 984-VT2BF-180	110	5	ditto
D	Tanker	234.00×37.00×19.80	88,461	Hitachi B&W 984-VT2BF-180	108	5	ditto
E	Ore Carrier	195.00×27.40×16.65	39,905	Hitachi B&W 784-VT2BF-180	110	5	ditto
F	Tanker	246.00×40.20×21.80	100,800	Hitachi B&W 1084-VT2BF-180	108	5	Tower Bridge
G	Tanker	207.00×31.84×14.50	45,250	Hitachi B&W 784-VT2BF-180	110	5	Conventional Type Superstructure
H	Tanker	265.00×44.20×21.50	121,450	Hitachi B&W 1284-VT2BF-180	108	5	Tower Bridge
I	Tanker	227.00×36.50×16.40	66,300	Hitachi B&W 884-VT2BF-180	108	5	Conventional Type Superstructure

simultaneously. Fig. 1 shows, as an example, the measuring locations on board ship D.

2.3 *Measurements and Results.*

2.3.1 Natural Frequencies of Superstructure.

The natural frequencies of fore-and-aft vibration of the superstructures are easily derived from the results of resonance measurements of the above-described full-scale tests. The observed natural frequencies are shown in Table 3. It is noticed that there are a good many small peaks between the prominent peaks in the observed resonance curves, but only the prominent are taken up in Table 3, and are provisionally named as the first mode, the second and the third counting from the lowest frequency.

From Table 3 it is learned that the lowest natural frequency seems to decrease as the number of decks of superstructure increases, and the superstructure with six or seven decks has the possibility of resonating with the blade frequency. Fig. 2 shows the relation between the number of decks and the lowest natural frequency.

Table 4 shows the values of N_2/N_1 and N_3/N_1, where N_1, N_2, and N_3 are the observed natural frequencies of the first, second and third mode respectively. As well known, the values of N_2/N_1 and N_3/N_1 in shear vibration of a uniform cantilever beam are 3.0 and 5.0 respectively, but they are far from the observed shown in Table 4.

2.3.2 Vibration Mode Curve of Superstructure.

One of the vibration mode curves of the superstructures obtained on the full-scale vibration measurements are shown, for an example, in Fig. 3. These curves are represented in non-dimensional form by dividing the vibration amplitude at each measuring point by that at the top deck of superstructure. It is seen from these curves that though slight descrepancies exist at the lower parts of superstructures, there is no remarkable difference in the shapes of the mode curves between the first and second modes and that even the upper deck of the test ship on which

Table 2 Principal Particulars of Superstructure.

(m)

Ship Name	No. of Deck Layers	h_n	$h_1 \sim h_{n-1}$	$a_1 \times b_1$	$a_2 \times b_2$	$a_3 \times b_3$	$a_4 \times b_4$	$a_5 \times b_5$	$a_6 \times b_6$	$a_7 \times b_7$
A	6	2.7	2.6	7.2 × 9.4	7.2 × 9.4	7.2 × 9.4	31.8 × 18.8	37.7 × 21.2	37.7 × 18.8	—
B	6	2.7	2.65	7.1 × 7.0	7.1 × 11.4	8.3 × 16.4	18.8 × 16.4	29.6 × 18.8	35.9 × 18.8	—
C	6	2.6	2.6	7.2 × 9.135	8.1 × 10.4	8.1 × 22.0	32.73 × 35.0	34.66 × 30.4	48.27 × 35.0	—
D	6	2.6	2.6	9.0 × 7.5	9.0 × 12.2	9.0 × 12.2	24.3 × 16.4	29.7 × 21.2	54.03 × 23.6	—
E	5	2.7	2.6 ~ 2.45	9.5 × 10.0	9.5 × 16.0	28.0 × 22.0	28.0 × 20.0	43.0 × 26.0	—	—
F	7	2.7	2.6	7.2 × 10.8	7.2 × 14.4	7.2 × 14.4	9.0 × 27.0	10.8 × 28.8	13.5 × 8.2	13.5 × 11.28
G	6	2.6	2.6	8.5 × 11.0	8.5 × 16.0	9.8 × 18.4	27.0 × 21.0	33.2 × 21.0	46.0 × 31.8	—
H	7	2.7	2.6	7.2 × 10.8	7.2 × 14.4	7.2 × 14.4	9.0 × 27.0	10.8 × 28.8	13.5 × 8.2	13.5 × 11.28
I	6	2.7	2.6 ~ 2.45	9.5 × 10.0	9.5 × 10.0	9.5 × 16.4	27.8 × 22.4	28.9 × 20.0	42.5 × 25.6	—

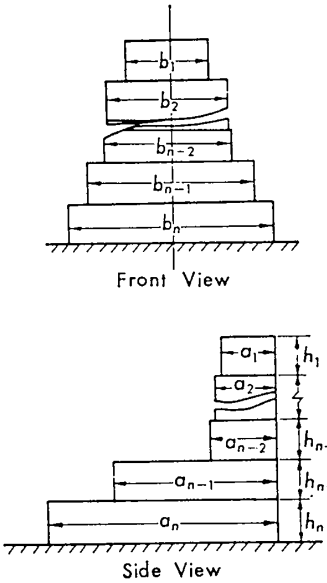

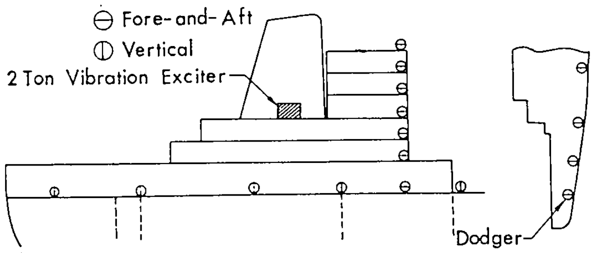

Fig. 1 Arrangement of Measuring Points (Ship D).

the superstructure is erected vibrates in fore-and-aft direction. This fact means that the superstructure cannot be considered to be a simple cantilever.

2.3.3 Vibration of Dodger.

Dodgers of the navigation bridge deck which overhang up to both shipside showed somewhat interesting vibratory behaviors on the full-scale vibration measurements. Fig. 4 shows an example of observed phase relations between dodger and superstructure at typical measuring points. From this figure it is noticed that dodger and superstructure vibrate in phase at lower frequencies, but in opposite phase at higher frequencies over 750 c/m.

Fig. 5 shows the observed mode patterns of the dodgers themselves. The patterns are represented in non-dimensional form by dividing the vibration amplitude at each measuring point of the dodger by that at the center line of the navigation deck. It is also found in this figure that in respect to amplitude, the dodger end does not differ much from the center line at the lower frequency and they vibrate in phase, but the end much exceeds the center line at the higher frequency and they oscillate in opposite phase.

2.3.4 Correlative Vibration between Ship's Hull and Superstructure.

It is wellknown that the fore-and-aft vibration of a superstructure of the kind in question is caused by the so-called hinging move-

Table 3 Observed Natural Frequency. (cpm)

Ship Name	1st Mode		2nd Mode		3rd Mode		Note
	Shaker Test	Trial	Shaker Test	Trial	Shaker Test	Trial	
A	—	525	—	720	—	—	1st test
	558	—	740	—			2nd test
B	—	558	783	776	950	994	
C	—	560	—	—	—	—	Trial only
D	550	555	650	637	860	—	
E	895	—	992	992	—	—	
F	440	443	500	490	990	—	Shaker tests were carried out twice
G	595	588	900	—	1050	—	
H	450*	430	783*	800	985*	—	* Values under construction
I	525	—	630	—	980	—	

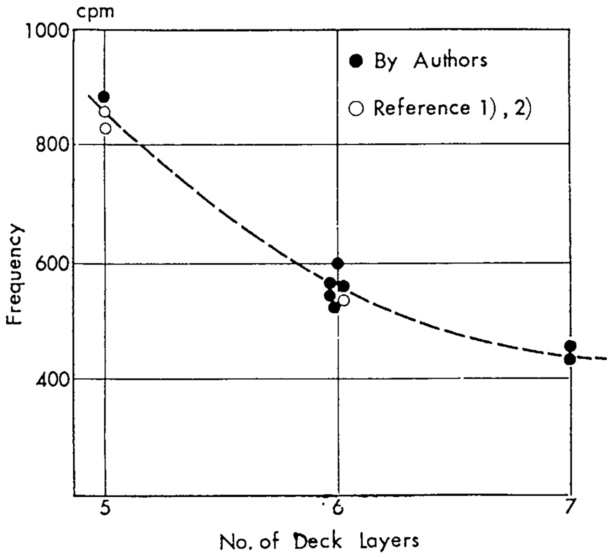

Fig. 2 Relation between Lowest Frequency and No. of Decks.

Table 4 Value of N_n/N_1

Ship Name	A	B	D	E	F	G	H	I
N_2/N_1	1.37 1.31	1.39	1.18 1.15	1.11	1.14	1.51	1.74	1.20
N_3/N_1	—	(1.70)	1.56	—	2.25	1.76	2.18	1.87

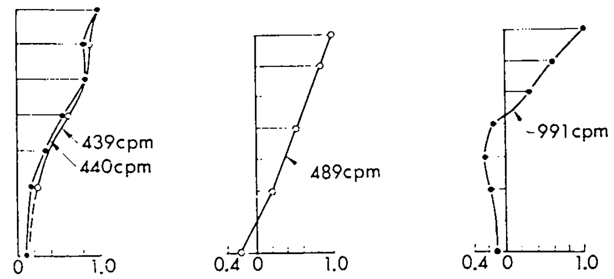

Fig. 3 Mode Curve of Superstructure.

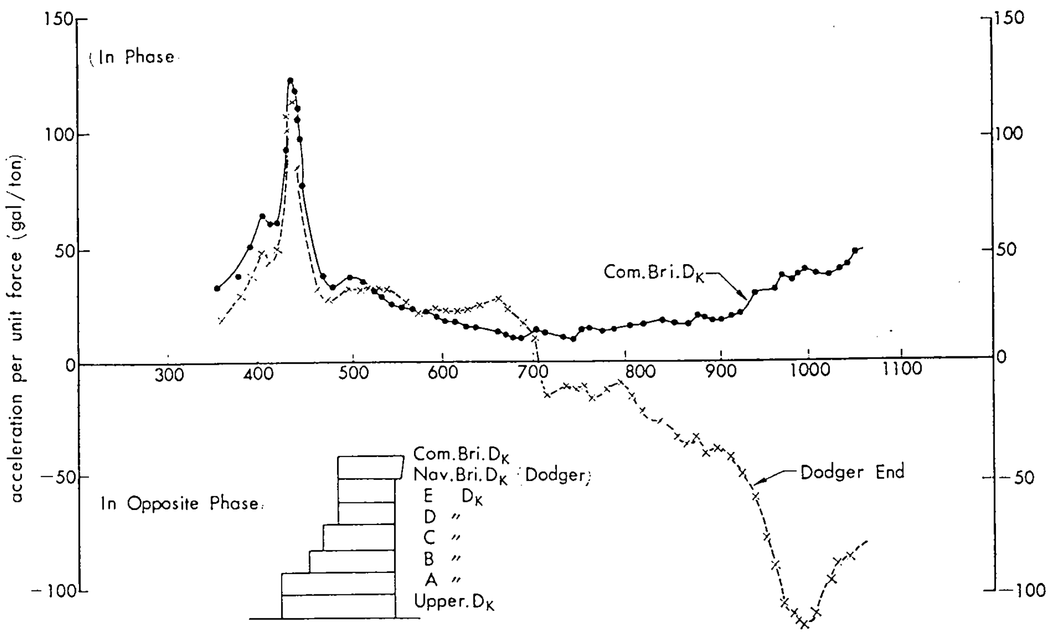

Fig. 4 Phase Relation between Dodger and Superstructure.

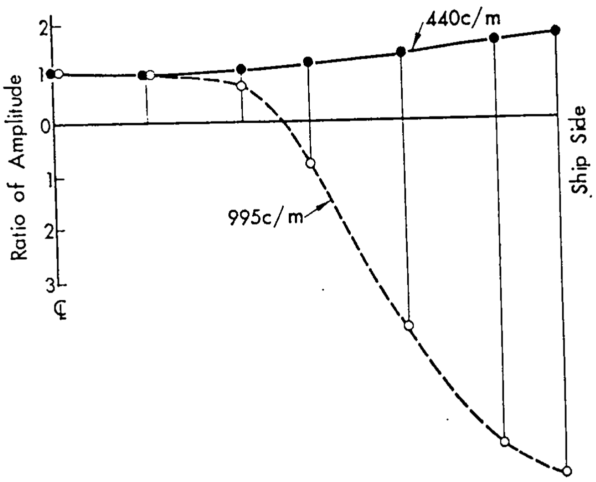

Fig. 5 Observed Mode Curve of Dodger.

ment due to the vertical flexural vibration of ship's hull. But recently the possible existence of the longitudinal vibration of ship's hull was pointed out and the hull vibration of this kind is said to affect on the vibratory characteristics of superstructure.

In order to make clear this problem, the vibration of superstructure and ship's hull were simultaneously measured on Ship I. Figs. 6 and 7 show the results of the measurements carried out at a pier by means of a vibration exciter installed on the top deck of the superstructure. From these figures it is clear that the ship's hull vibrates longitudinally and there are four peaks observed in the resonance curves. Moreover, as shown in Fig. 7, the superstructure and ship's hull vibrate in phase at two lower resonant frequencies, but at two higher ones they oscillate in counterphase.

3. Qualitative Investigation on Vibration Characteristics of Superstructure

3.1 *Coupled Vibration of Superstructure and Ship's Hull.*

The superstructure is assumed to be a uniform cantilever beam attached at the after part of the ship which is also assumed to be a uniform beam free at both ends as shown in Fig. 8. Equations of motion for longitudinal vibration of ship's hull and shear vibration of superstructure are given respectively as follows:

$$T\frac{\partial^2 U}{\partial X^2}-m\frac{\partial^2 U}{\partial t^2}=0,\quad S\frac{\partial^2 y}{\partial x^2}-\mu\frac{\partial^2 y}{\partial t^2}=0, \tag{3.1.1}$$

where,

T: tensile rigidity of hull
U: longitudinal displacement of hull
X: length co-ordinate of hull
m: mass of hull per length
S: shear rigidity of superstructure
y: fore-and-aft displacement of superstructure
x: height co-ordinate of superstructure
μ: mass of superstructure per height.

Boundary conditions for free vibration are given in the followings:

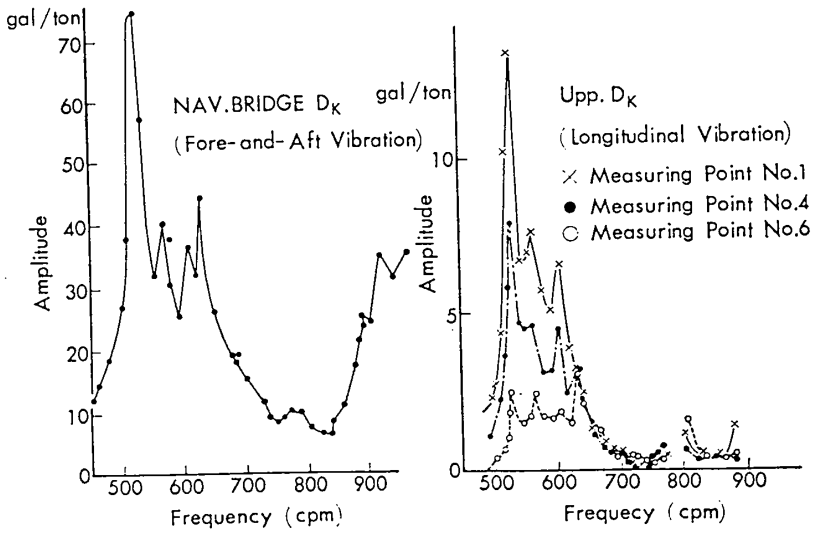

Fig. 6 Resonance Curve.

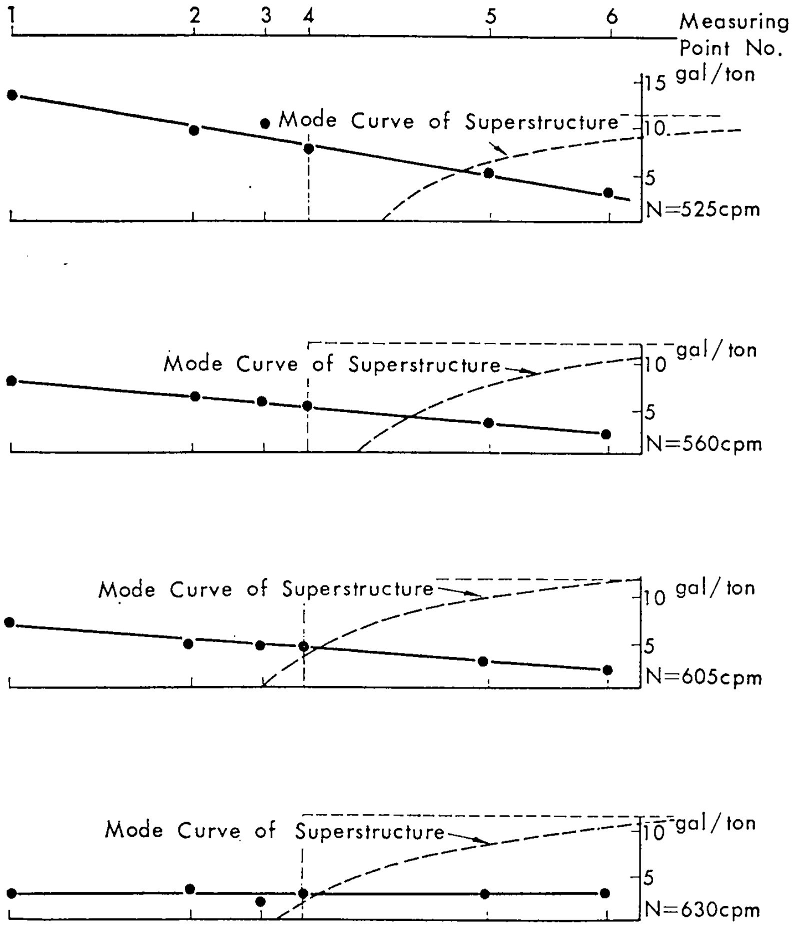

Fig. 7 Longitudinal Vibration Modes of Ship's Hull.

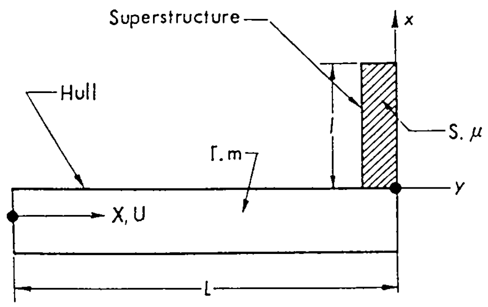

Fig. 8

$$\left.\frac{\partial U}{\partial X}\right|_{X=0}=0, \quad T\left.\frac{\partial U}{\partial X}\right|_{X=L}=S\left.\frac{\partial y}{\partial x}\right|_{x=0}$$
$$\left. y\right|_{x=0}=\left. U\right|_{X=L}, \quad \left.\frac{\partial y}{\partial x}\right|_{x=l}=0 \qquad (3.1.2),$$

where,

L: length of ship
l: height of superstructure

For the forced vibration excited by a periodic force acting at the top of superstructure, the last equation of (3.1.2) is replaced by

$$\left.\frac{\partial y}{\partial x}\right|_{x=l}=\frac{F_0}{S}e^{i\omega t} \qquad (3.1.2)',$$

where,

F_0: amplitude of exciting force
ω: circular frequency of exciting force.

U and y are expressed in the following forms.

$$\left.\begin{aligned} U&=(A_1e^{iKX}+A_2e^{-iKX})e^{i\lambda t}\\ y&=(A_3e^{ikx}+A_4e^{-ikx})e^{i\lambda t}\end{aligned}\right\} \qquad (3.1.3)$$

And by using (3.1.1), (3.1.2) and (3.1.3), the following equation is given for the characteristic values of natural frequencies:

$$\tan KL=-\alpha \tan kl \qquad (3.1.4)$$

Amplitudes of the forced vibration are

given by replacing $e^{i\lambda t}$ with $e^{i\omega t}$ in U and y of (3.1.3) and obtaining the general solution of (3.1.1) under the conditions of (3.1.2), (3.1.2)′ and (3.1.3) as follows:

$$U=\frac{\alpha(1-1/\cos kl)\cos KX/\cos KL}{\tan KL+\alpha\tan kl}Qe^{i\omega t} \tag{3.1.5}$$

$$y=\frac{\{\alpha(1-1/\cos kl)\cos k(l-x)+(\tan KL+\alpha\tan kl)\sin KX\}/\cos kl}{\tan KL+\alpha\tan kl}Qe^{i\omega t} \tag{3.1.6}$$

where,

$$\alpha=\frac{w}{\Delta}\cdot\frac{KL}{kl}=\frac{w}{\Delta}\beta,\quad Q=E_0/kS$$

Δ: weight of ship
w: weight of superstructure

The ratio of the amplitude at the top of the superstructure to the amplitude at its bottom is given according to (3.1.6) by

$$\frac{y_l}{y_0}=\frac{1}{\cos kl}+\frac{\tan KL+\alpha\tan kl}{\alpha(1-1/\cos kl)}\tan kl \tag{3.1.7}$$

where,
y_l: amplitude at top of superstructure
y_0: amplitude at bottom of superstructure.

If it is assumed as an example that $T=80\times10^6$ tons, $\Delta=30{,}000$ tons, $L=200$ m, $S=10^6$ tons, $w=300$ tons and $l=18$ m, the natural frequency of the superstructure and the ship's hull are 420 c/m and 450 c/m respectively, but the coupled natural frequencies calculated from the above-described formula are 400 c/m and 470 c/m, so two resonant frequencies will exist in U and y. And for 400 c/m, $(y_l/y_0)>0$ that is to say y_l and y_0 are in phase, but for 470 c/m, $(y_l/y_0)<0$ that is to say y_l and y_0 are in opposite phase.

These analytical investigations show qualitatively the reason why there are near 500~600 c/m on ships more than two resonant frequencies which have the nature that at the lower frequencies the superstructure and ship's hull vibrate in phase but at the higher frequencies they oscillate in opposite phase.

As shown in Fig. 6, four resonant frequencies are observed in the vicinity of first mode on the full-scale vibration measurements on Test Ship I. These phenomena are explained by the following considerations. As previously described, both longitudinal vibration and vertical flexural vibration of ship's hull affect the vibratory behaviors of the superstructure. Therefore, two of the above-mentioned four peaks may be caused by the correlative vibration with the ship's hull longitudinal vibration, and the other two by that with the ship's hull vertical flexural vibration.

In evaluation of the change rate of the characteristic number of natural frequency due

Table 5 β VS. kl and N_2/N_1

β	$(kl)_1$	$(kl)_2$	N_2/N_1
3.00	1.57(1.00)	2.12(1.36)	1.36
3.25	1.55(0.99)	1.95(1.24)	1.25
3.50	1.53(0.98)	1.79(1.14)	1.16
3.75	1.50(0.97)	1.73(1.10)	1.13
4.00	1.48(0.94)	1.66(1.05)	1.12
4.25	1.45(0.92)	1.64(1.03)	1.12
4.50	1.39(0.89)	1.61(1.02)	1.15
4.75	1.32(0.84)	1.59(1.01)	1.20
5.00	1.22(0.78)	1.57(1.00)	1.28

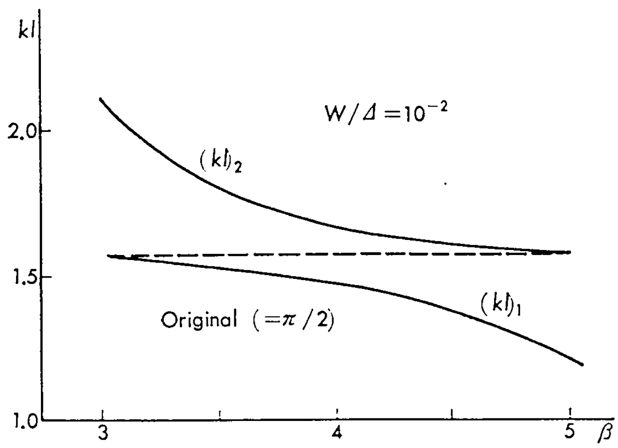

Fig. 9 β V.S. kl.

to the effects of correlative vibration with ship's hull, Eq. (3.1.4) is available. The relation between β and kl is evaluated by (3.1.4) and is given in Fig. 9 and Table 5. The quantity β for an actual ship is supposed to be near 4.00, therefore, it is clear from Fig. 9 and Table 5 that the deviations of kl from the original value are between $\pm 5\%$ and and the value of N_2/N_1 becomes 1.12 approximately. The value of N_2/N_1 thus evaluated has the same order as the observed values on the full-scale vibration measurements.

However, as described in detail later, when the first mode natural frequency of the superstructure is calculated on the assumption that the superstructure is a cantilever with variable cross section, it is almost 100% in excess of the observed on the full-scale tests. Therefore, the above-mentioned argument alone cannot explain the discrepancy between the calculated and observed natural frequencies.

3.2 *Effect of Boundary Condition.*

In this paragraph the effects of boundary conditions of superstructures on the natural frequencies are investigated. Fig. 10 shows the simplification of the vibrating system applied for the investigation.

The latter part of Eq. (3.1.1) is available for the equation of motion for this case, and the boundary conditions are given as follows:

$$\left.\frac{\partial y}{\partial x}\right|_{x=0}=\frac{K_1}{S}y\Big|_{x=0},\quad \left.\frac{\partial y}{\partial x}\right|_{x=l}=0 \qquad (3.2.1).$$

The equation of the characteristic number of natural frequency is given from (3.1.1), (3.1.3) and (3.2.1),

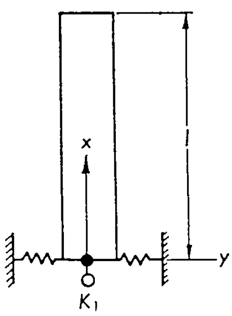

Fig. 10

Table 6 ε VS. kl and N_2/N_1

ε	$(kl)_1$	$(kl)_2$	N_2/N_1
0	1.57(1.00)	4.70(1.00)	3.00
0.1	1.45(0.92)	4.31(0.92)	3.01
0.3	1.22(0.78)	3.86(0.82)	3.16
0.5	1.06(0.68)	3.63(0.77)	3.42
1.0	0.87(0.56)	3.40(0.72)	3.91

$$\cos kl-\frac{1}{q}\sin kl=0 \qquad (3.2.2),$$

where,

$$q=K_1/kS$$

K_1: spring constant of elastic support at foundation of superstructure.

Table 6 got by computing graphically from (3.2.2), shows the change of the characteristic number kl and of N_2/N_1 with respect of ε, where ε equals S/k_1l. It is clear from this Table that along with the increase of ε, namely the decrease of K_1, the characteristic number decreases, but N_2/N_1 increases. From this fact it may be understood that the remarkable discrepancy between the calculated and observed natural frequencies of the first mode is mainly due to the existence of elastic supports at the foundation deck of superstructure. But the idea of introducing the elastic supports cannot be a complete proof for the discrepancy of the value of N_2/N_1, for the computed values of N_2/N_1 increases along with the decrease of K_1 and are far from the observed one.

3.3 *Effect of Dodger Vibration.*

According to the results of full-scale vibration tests, it is presumed that dodgers affect to some extent the vibratory behaviors of superstructure. In order to make clear this effect, the following investigation was made. As shown in Fig. 11, the dodger is assumed to be a sprung mass attached to superstructure.

Then the periodic force induced by the sprung mass to superstructure is expressed by the following equation:

$$f=K_2y_2|_{x_2=0}$$

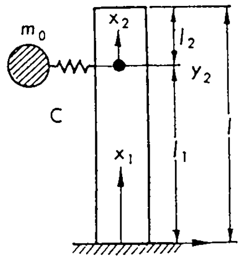

Fig. 11

where,

$$K_2 = C\omega^2/(\sigma^2-\omega^2)$$

$\sigma=\sqrt{C/m_0}$: natural circular frequency of sprung mass

ω: circular frequency of vibration.

For the equation of motion of superstructure beam, the latter part of (3.1.1) is available and the boundary conditions are given as follows:

$$\left.\begin{aligned} &y_1|_{x_1=0}=0, \quad \left.\frac{\partial y_1}{\partial x_1}\right|_{x_1=l_1} = \left.\frac{\partial y_2}{\partial x_2}\right|_{x_2=0} + \frac{K_2}{S}y_2\bigg|_{x_2=0}, \\ &y_1|_{x_1=l_1}=y_2|_{x_2=0}, \quad \left.\frac{\partial y_2}{\partial x_2}\right|_{x_2=l_2}=0 \end{aligned}\right\} \tag{3.3.1}$$

Expressing the displacement of superstructure y_j $(j=1, 2)$ by the following equation:

$$y_j=(A_je^{ikx_j}+B_je^{-ikx_j})e^{i\lambda t} \quad (3.3.2).$$

Then the equation of characteristic number is given by

$$\cos kl = R \sin kl_1 \cos kl_2 \quad (3.3.3),$$

where,

$$R=K_2/kS, \quad l=l_1+l_2$$

When the natural circular frequency of the sprung mass $\sigma\ (=\sqrt{c/m_0})$ is assumed to be η times the second mode natural circular frequency of superstructure $\lambda\left(=\frac{3\pi}{2l}\sqrt{\frac{S}{\mu}}\right)$, the following equation is obtained:

$$\omega/\sigma=2kl/3\pi\eta,$$

and then

Table 7 η VS. N_n/N_1 $(\xi=0.1)$

η	N_2/N_1 $l_1/l=0.8$	N_2/N_1 $l_1/l=1.0$	N_3/N_1 $l_1/l=0.8$	N_3/N_1 $l_1/l=1.0$
4/3	3.00	2.77	4.50	4.30
1	2.89	2.65	3.65	3.85
2/3	2.38	2.62	3.28	3.58
1/2	1.87	1.75	3.43	3.58
0	3.00		5.00	

$$R=\xi kl/\{1-(2kl/3\pi\eta)^2\} \quad (3.3.4),$$

where,

$\xi=m_0/\mu L$: mass ratio of sprung mass attached to superstructure and superstructure.

(3.3.3) can be easily solved graphically and Table 7 shows the values of N_n/N_1 affected by the dodger as the sprung mass when $\xi=0.1$. This table indicates that N_n/N_1 decreases along with the decrease of η, and in the range of $\eta=1/2\sim2/3$, it becomes the same order as the observed N_3/N_1.

3.4 *Main Results of Qualitative Investigation.*

Qualitative investigations were made on the vibratory characteristics of superstructures, especially on the correlation between superstructure vibration and ship's hull vibration, on the effects of boundary conditions of super-

Table 8 Qualitative Analysis of Natural Frequency of Superstructure

	N_1(c/m)	N_2(c/m)
Calculated frequency for a variable section cantilever	1,000	3,000
Frequency affected by elastic support (assumed $\varepsilon=0.5$)	680	2,310
Frequency affected by sprung mass (assumed $\xi=0.1$, $\eta=0.5$, $l_1=l$)	590	1,250·2,400
Frequency affected by lougitudinal hull vibration (assumed $\beta=4.0$)	555 · 620	1,170·1,310

structure foundations and on the sprung mass effect of the dodger. They appear to affect jointly and simultaneously the vibration of superstructures, and will be discussed separately later. Taking into consideration of these joint effects, the natural frequencies of fore-and-aft vibration of superstructures are analyzed qualitatively as shown in Table 8. The last natural frequencies shown in the table are not far from the observed frequencies.

4. Prediction of Lowest Natural Frequency

In order to prevent the trouble of fore-and-aft vibration of superstructure, it is necessary to predict its natural frequency in the early stage of designing and avoid the resonance with external periodic forces. As already stated, only the lowest of the natural frequencies of superstructures has a possibility to resonate with external forces.

The vibratory behaviors of superstructure are very complicated because of the existence of correlations with the ship's hull, sprung mass effects and elastic supports, but fortunately the effects of the former two upon the lowest natural frequency are relatively small.

Therefore, to predict the lowest natural frequency of superstructure, it is sufficient for practical use to take into consideration only of the effects of elastic supports.

4.1 *Assumption for Calculation.*

To develop the method which predicts the critical frequency, the following assumptions are made:

(1) The superstructure is considered as a multi-sprung-mass vibratory system with n degrees of freedom, where n is the number of its deck layers.

(2) Viscous damping and rotational inertia are neglisibly small.

(3) The shear rigidity and bending rigidity alone of superstructure bulkheads are taken into the spring of the multi-sprung-mass system. The rigidity of deck plate is neglisible.

(4) The weights of steel plating and fittings are replaced into the vibratory mass of the multi-sprung-mass system. The weights are assumed to concentrate on each deck layer on which they are erected.

(5) The displacement of superstructure is the sum of shear deflection, bending deflection and deflection due to the elasticity of the foundation deck.

4.2 *Equation of Motion*

For the multi-sprung-mass vibratory system, the following relations exist between displacement, external force and inertia force.

$$\boldsymbol{Y}=\boldsymbol{\Phi P}=-\boldsymbol{\Phi M}\ddot{\boldsymbol{Y}}=-\boldsymbol{U}\ddot{\boldsymbol{Y}} \quad (4.2.1),$$

$\boldsymbol{Y}$: displacement (column matrix)
$\boldsymbol{P}$: external force (column matrix)
$\boldsymbol{\Phi}$: flexibility matrix (symmetric matrix of order n)
$\boldsymbol{M}$: inertia matrix (diagonal matrix)
$\boldsymbol{U}$: dynamical matrix (regular square matrix).

In the case of a vibratory motion, $\boldsymbol{Y}$ is expressed by the following equation:

$$\boldsymbol{Y}=e^{i\omega t}\boldsymbol{A} \quad (4.2.2).$$

Eqs. (4.2.1) and (4.2.2) give the following equation:

$$\left(\frac{1}{\omega^2}\boldsymbol{I}_n-\boldsymbol{U}\right)\boldsymbol{A}=0 \quad (4.2.3),$$

where,

ω: circular frequency
$\boldsymbol{I}_n$: unit matrix of order n
$\boldsymbol{A}$: modal column matrix.

In order to solve the above equation by means of the socalled "Repitition Method", presume $\boldsymbol{A}$ to be

$$\boldsymbol{A}={}_0A\begin{pmatrix}{}_0A_1\\ {}_0A_2\\ \vdots\\ {}_0A_n\end{pmatrix} \quad (4.2.4),$$

and substitute this in (4.2.3), then the following equation is obtained:

$$\frac{1}{\omega^2}\begin{pmatrix} {}_0A_1 \\ {}_0A_2 \\ \vdots \\ {}_0A_n \end{pmatrix} = U\begin{pmatrix} {}_0A_1 \\ {}_0A_2 \\ \vdots \\ {}_0A_n \end{pmatrix} = \begin{pmatrix} {}_0A'_1 \\ {}_0A'_2 \\ \vdots \\ {}_0A'_n \end{pmatrix}$$

$$= \frac{{}_0A'_1}{{}_0A_1}\begin{pmatrix} {}_0A_1 \\ {}_0A'_2\dfrac{{}_0A_1}{{}_0A'_1} \\ \vdots \\ {}_0A'_n\dfrac{{}_0A_1}{{}_0A'_1} \end{pmatrix} = \frac{{}_0A'_1}{{}_0A_1}\begin{pmatrix} {}_1A_1 \\ {}_1A_2 \\ \vdots \\ {}_1A_n \end{pmatrix} \tag{4.2.5}$$

When this process is repeated n times, the sequence of ${}_0A'_1/{}_0A_1$, ${}_1A'_1/{}_1A_1 \cdots {}_nA'_1/{}_nA_1$ converges to a certain value and the convergent value corresponds to $1/\omega^2$. The lowest natural frequency of the system is given by

$$f = \frac{60}{2\pi}\sqrt{\frac{{}_nA_1}{{}_nA'_1}} \tag{4.2.6}$$

4.3 *Evaluation of Flexibility Matrix.*

For the above-described calculation, it is necessary to evaluate both Inertia Matrix M and Flexibility Matrix Φ. The Inertia Matrix M can be easily evaluated by the following formula:

$$M = \begin{pmatrix} m_1 & 0 & 0 & \cdots & 0 \\ 0 & m_2 & 0 & \cdots & 0 \\ 0 & 0 & m_3 & \cdots & 0 \\ \cdots & \cdots & \cdots & \cdots & \cdots \\ 0 & 0 & 0 & \cdots & m_n \end{pmatrix}, \tag{4.3.1}$$

where,

m_j: vibratory mass on jth deck of superstructure ($j=1, 2, \cdots n$, counted from top.).

Evaluation of Flexibility Matrix is fairly complicated, but it is divided into the following three matrices.

- ${}_s\Phi$: flexibility matrix due to shear
- ${}_b\Phi$: flexibility matrix due to bending
- ${}_r\Phi$: flexibility matrix due to elastic support at foundation deck (generally upper deck)

Evaluations of these matrices are shown in detail in reference[8], and they are expressed finally as follows:

$$ {}_s\Phi = \frac{l}{G}{}_s\Phi' = \frac{l}{G}[{}_sL_1\boldsymbol{\alpha},\ {}_sL_2\boldsymbol{\alpha},\ \cdots\ {}_sL_n\boldsymbol{\alpha}] \tag{4.3.2}$$

where,

$$ {}_sL_i = \begin{pmatrix} 00\cdots01 & & \cdots11 \\ 00\cdots01 & \Big\} 1\times i \text{ at } i\text{th row} & \cdots11 \\ \cdots\cdots & & \cdots\cdots \\ \cdots\cdots01 & & \cdots\cdots \\ \cdots\cdots00\cdots\cdots & & \\ \cdots\cdots\cdots\cdots & & \\ 00\cdots00\cdots11 & & \\ 00\cdots00\cdots01 & & \end{pmatrix}, \quad (n \text{ rows})$$

$$\boldsymbol{\alpha} = \begin{pmatrix} 1/k'A_1 \\ 1/k'A_2 \\ \vdots \\ 1/k'A_n \end{pmatrix}$$

- G: modulus of shear elasticity
- $k'A_i$: effective cross sectional area for shear
- l: deck height.

$$ {}_b\Phi = \frac{l^3}{6E}{}_b\Phi' = \frac{l^3}{6E}[{}_bL_1\beta,\ {}_bL_2\beta,\ \cdots\ {}_bL_n\beta] \tag{4.3.3}$$

where,

$$ {}_bL_i = \begin{pmatrix} 00\cdots0S(i-1,0), \cdots & S(n-1,n-i) \\ 00\cdots0S(i-2,0), \cdots & S(n-2,n-i) \\ \cdots\cdots\cdots\cdots & \cdots\cdots \\ \cdots\cdots\ S(0,0) & \cdots\cdots \\ \cdots\cdots\ 0 & \cdots\cdots \\ \cdots\cdots\cdots\cdots & \cdots\cdots \\ 00\cdots\ 0\ \cdots & S(0,n-i) \end{pmatrix},$$

$$\beta = \begin{pmatrix} 1/I_1 \\ 1/I_2 \\ \vdots \\ 1/I_n \end{pmatrix}$$

$$S(u, v) = 6uv + 3(u+v) + 2$$

E: Young's modulus
l: deck height
I_i: moment of inertia of cross section at ith deck.

$$_r\Phi=\frac{l}{\gamma}{}_r\Psi \qquad (4.3.4),$$

where,

$$_r\Psi=\begin{pmatrix} n^2 & (n-1)n & \cdots & 2n & n \\ n(n-1) & (n-1)^2 & \cdots & 2(n-1) & (n-1) \\ \cdots & \cdots & \cdots & \cdots & \cdots \\ 2n & (2n-1) & & 2^2 & 2 \\ n & (n-1) & & 2 & 1 \end{pmatrix}$$

γ: rotational spring constant at the foundation deck
l: deck height

4.4 *Discussion of Validity of Proposed Method.*

In order to study the validity of the proposed method, comparisons between the observed and calculated natural frequencies were made. Natural frequencies were calculated by means of an electronic digital computer HITAC 3010.

4.4.1 Comparison between Observed and Calculated Natural Frequency.

The calculated natural frequency of shear vibration of superstructure is compared with observed in Table 9. This table tells that the calculated natural frequency is about 70~100% higher than the observed.

Table 9 Comparison between Calculated and Observed ($K=\infty$)

Ship Name	Calculated N_c	Observed N_m	N_c/N_m
A	1,016	525	1.93
B	983	558	1.76
C	958	550	1.74
D	1,097	550	1.99
F	727	440	1.66

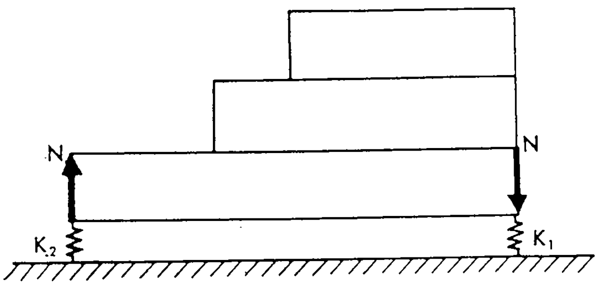

Fig. 12 γ

4.4.2 Effect of Elastic Support at Foundation Deck.

It is somewhat difficult to evaluate directly the spring constant of foundation deck, and a simplification was applied in the system as shown in Fig. 12. The superstructure is assumed to be supported with two springs at the bottoms of its fore and aft end bulkheads. Then the following equation is obtained:

$$\gamma=\frac{M_0}{\theta}=\frac{K_1K_2}{K_1+K_2}a^2=Ka^2 \qquad (4.4.1),$$

where,
a: distance between fore and aft end bulkheads
M_0: moment due to vertical force
K: equivalent spring constant
K_1: spring constant for fore end bulkhead
K_2: spring constant for after end bulkhead
θ: rotational angle due to moment

To evaluate the values of K_1 and K_2, the following assumptions were made.

(1) The vertical force from the superstructure is transmitted to bulkheads (transverse and longitudinal) under the foundation deck.

(2) The bulkheads under the foundation deck which have a bulkhead undernearth in the same vertical plane act only in compression.

(3) The bulkheads under the foundation deck which have not a bulkhead undernearth in the same vertical plane act both in compression and in shear. The compression is supposed to act in one-frame-space breadth.

(4) The rigidity of deck plating of all superstructure decks is neglected.

(5) Spring constants of the foundation deck are derived by calculations of displacements, and the calculated spring constants of each deck are summed up. The sums make the equivalent spring constants K_1 and K_2 for the vertical planes under the superstructure bulkheads forward and aft.

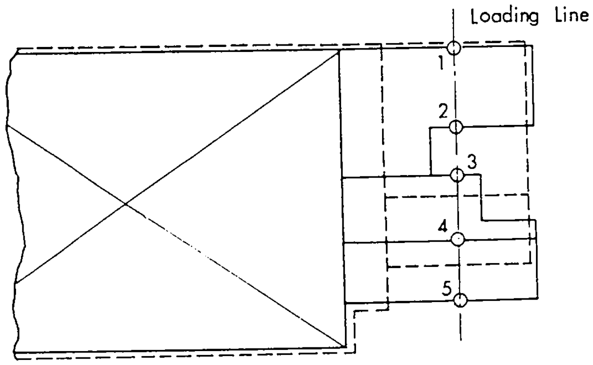

Fig. 13 An Example of House Wall Arrangement.

The calculation of the spring constant is, as an example, shown as follows: Fig. 13 is a plan of deck just below the foundation deck, showing the superstructure after end in a chain line and bulkheads below this deck in broken lines. The vertical force from the superstructure after end bulkhead acts upon the intersections of the chain line, and these are named Points 1, 2,...5 as shown in the figure. On the above-described assumptions, the following calculations are made.

$$K_{1C}=\frac{AE}{l}=\frac{150\times 0.6\times 2100}{260}$$
$$=726.9 \text{ t/cm},$$
$$K_{2C}=K_{3C}=K_{4C}=K_{5C}=\frac{AE}{l}$$
$$=\frac{90\times 0.6\times 2100}{260}=436.2 \text{ t/cm},$$
$$K_{2S}=K_{3S}=K_{4S}=\frac{L}{L_1L_2}kAG=\frac{330}{180\times 150}$$
$$\times 260\times 0.6\times 820=1{,}563.5 \text{ t/cm},$$
$$K_{5S}=\frac{480}{180\times 300}\times 260\times 0.6\times 820$$
$$=1{,}137.1 \text{ t/cm},$$

where,

l: deck height
A: sectional area ($d\times t$)
d, L: span
t: plate thickness
K_{nC}: compressive spring constant ($n=1, 2, \cdots 5$)
K_{nS}: shear spring constant ($n=1, 2, \cdots 5$)
E: Young's modulus
kAG: shear rigidity
L_1, L_2: distance from loading point to support.

Therefore,

$$K_2'=K_3'=K_4'=1/(1/436.2+1/1563.5)$$
$$=341.0 \text{ t/cm}$$
$$K_5'=1/(1/436.2+1/1137.1)=315.2 \text{ t/cm}$$
$$K=K_{1C}+K_2'+K_3'+K_4'+K_5'=2065 \text{ t/cm}$$

Table 10 Natural Frequency (cpm)

Ship Name	A	B
Calculated N_c	535	405
Observed N_m	525 (558)*	440
N_c/N_m	1.02 (0.96)*	0.92

( )* shows value of 2nd Test.

4.4.3 Calculated Natural Frequency taking account of Elastic Supports.

The above-described calculations of natural frequencies were made on Ships A and F. Table 10 shows the calculated natural frequency of superstructure by taking into account the elastic supports at the foundation deck. It is known from this table that the discrepancies between the calculated and observed became considerably smaller than those shown in Table 9 when the elastic support is taken into account.

5. Conclusion

The results of the full-scale measurements and the investigations thereof are summarized as follows:

(1) There are several resonant frequencies of 400~600 c/m and 800~1,000 c/m in the resonance curves obtained. Of these, the lowest natural frequency has the possibility of resonating with the so-called "blade frequency".

(2) The observed mode curves of superstructure and dodger show some interesting characteristics. That is, the former give nearly the same shapes in the first and the second modes, and the latter give different vibration

phases in the first and the second modes.

(3) The existence of correlative vibrations between main hull and superstructure is clearly recognized during the full-scale vibration tests.

(4) It is made clear that the elastic condition of fixing at the foundation deck of superstructure makes the natural frequencies decrease remarkably, and the sprung mass effects of the dodgers affect the natural frequencies of the second mode.

(5) In the proposed method which determines the lowest natural frequency, the evaluation of *K*-value is most important.

References

1) "On the Vibration of After Bridge." by Kure Dock Yard. Report to Shipstructure Committee, the Society of Naval Architects of West Japan. (Sept. 1964)

2) "On the Natural Frequency of Superstructure." by Kawasaki Dock Yard. Report to Shipstructure Committee, the Society of Naval Architects of West Japan. (Oct. 1965)

3) "Some Observations and Preventing Method of Ship Vibration." by T. HIROWATARI and M. FUJIWARA. Journal of Kansai Society of Naval Architects, Japan. No. 96 (Dec. 1959)

4) "On the Vibration of After Bridge." by T. KUMAI. Report to Shipstructure Committee, the Society of Naval Architects of West Japan. (Oct. 1965)

5) "On the Longitudinal Main Hull Vibration." by Y. WATANABE. Report to Shipstructure Committee, the Society of Naval Architects of West Japan. (Oct. 1960)

6) "On the Vibration of Desh Bandu," by H. OHSHIMA. Report of Hitachi Shipbuilding and Engineering Co. (Nov. 1964)

7) "On the Causes of The Stern Vibration of a Ship." by Y. WATANABE. Journal of the Society of Naval Architects of West Japan. No. 20 (Nov. 1960)

8) "On the Fore-and-aft Vibration of Superstructure Located at Aftership." by T. HIROWATARI and K. MATSUMOTO. Journal of the Society of Naval Architects of Japan. Vol. 119 (June 1966)